Epitaxial growth and device fabrication of GaN based electronic and optoelectronic structures

S. Müller [1)] , R. Quay [1)] , F. Sommer [1)] , F. Vollrath [1)] , R. Kiefer [1)] , K. Köhler [1)] , J. Wagner [1)]
1) Fraunhofer−Institut für Angewandte Festkörperphysik, Tullastrasse 72, 79108 Freiburg, Germany

1.Introduction

At the Fraunhofer IAF both single and multiwafer low−pressure MOVPE reactors are used for the growth of a) GaN/AlGaN layer sequences for the fabrication of high electron mobility transistors (HEMTs) and b) complex GaInN/GaN/AlGaN layer structures for violet and UV LEDs as well as violet emitting diode lasers. In the following both growth related issues as well as results on devices fabricated from these epitaxial layer sequences will be discussed in section 2 for electronic devices and in section 3 for light emitting diodes and diode lasers.

2. AlGaN/GaN based HEMT

High electron mobility transistors (HEMTs) based on GaN/AlGaN heterostructures are well suited for high power microwave amplifiers covering the 2 – 40 GHz frequency range [1−3]. The main advantages of GaN over Si and GaAs stem from its wide bandgap, hence high breakdown field and high electron saturation velocity. This material offers large potential to surpass existing device limitations in RF output power, operation voltage and operation temperature. The HEMT structures can be grown either on sapphire or on s.i. SiC substrates. Sapphire is available at significantly lower costs and in larger sizes than SiC and is successfully used for optoelectronic devices (see below). However, to develop full RF performance, the dissipated power has to be removed as effectively as possible. Therefore s.i. SiC is the substrate of choice providing an excellent thermal conductivity of 3.5 W/cm·K, which is an order of magnitude higher than that of sapphire.

a) Epitaxy and characterization

The HEMT structures are grown in an AIXTRON 2000 G3 HT 6´2" multiwafer reactor. On SiC a 500 nm thick AlGaN layer is grown followed by a 2.75 µm thick highly insulating GaN buffer layer. The spontaneous and piezoelectric polarization of a 25 nm thick $Al_{0.25}$ $Ga_{0.75}$ N layer on top of the buffer results in a two−dimensional electron gas (2−DEG) at the GaN/AlGaN interface (Fig. 1) [4]. In Si−doped HEMT structures the Si−doped AlGaN supply layer is sandwiched between an undoped AlGaN spacer and barrier layer. The structure is capped with a 2 nm thick GaN layer. A similar layer sequence is used for the growth on sapphire. The Al−content and the AlGaN layer width of the actual HEMT structures are verified by spectral ellipsometry [5].

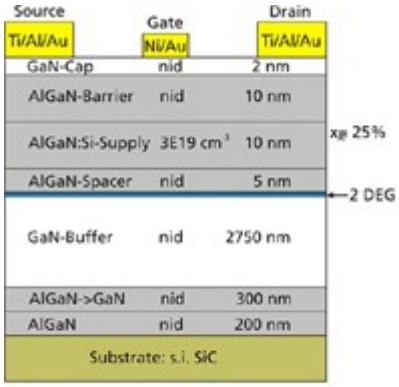

Fig. 1: Epitaxial layer structure of the GaN/AlGaN HEMT grown by MOVPE

The 2−DEG concentration for a HEMT−structure with an Al−content of 25 % can be increased from $4x10^{12}$ cm^{-2} to $1.5x10^{13}$ cm^{-2} by modulation doping, where the nominal Si−doping level varies from zero to $3x10^{19}$ cm^{-3}, respectively. The mobility of HEMT−structures on s.i. SiC is slightly higher than on sapphire for the same carrier concentration. From Hall measurements typical sheet carrier concentrations and electron mobilities of $8x10^{12}$ cm^{-2} and 1400 cm^2 /Vs were obtained. Sheet resistance (Rs) mappings across the wafers and from wafer to wafer proved an excellent uniformity. In Fig. 2 the Rs across a 2" SiC wafer is shown with an average value of 483 Ohm and a standard deviation of ± 0.6 %. Device structures were grown reproducibly over a 2 year period with a typical on−wafer standard deviation in Rs of 1 − 4 %. There is a trend towards devices with higher Al content in HEMT structures as this results in a higher sheet carrier density in the channel due to an increase in the spontaneous and piezoelectric polarization charge [4]. In addition the higher bandgap of the AlGaN layer promises a higher composite breakdown field. The influence of the increasing Al content from 25 % to 35 % is demonstrated in Fig. 3. We observe a linear increasing sheet carrier density and almost constant mobility for undoped HEMT structures. The highest mobility of 1500 cm^2 /Vs is achieved for a structure with an Al−content of 30 %.

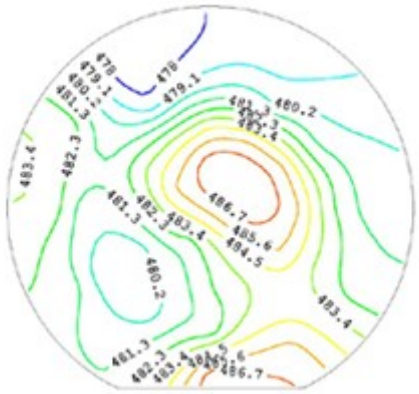

Fig. 2: Distribution of the Rs of a GaN/AlGaN HEMT-structure with x(Al)= 25 % on a 2" s.i. SiC substrate. Average Rs = 483 W ± 0.6 %.

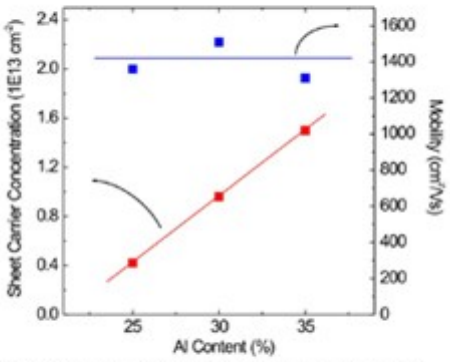

Fig. 3: Sheet carrier concentration and mobility ofundoped GaN/AlGaN HEMT structures on sapphire as a function of the Al content in the AlGaN layer.

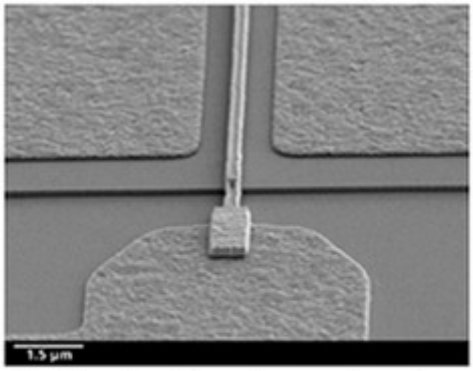

Fig. 4: Scanning electron microscope image of a HEMT with a gatelength lg = 150 nm.

b) Process technology and device performance

Device fabrication was done on full 2" wafers by contact lithography. Device isolation was accomplished by a 180 nm deep mesa dry etch into the GaN buffer by chemically assisted ion beam etching using chlorine. Ti/Al/Au alloyed ohmic contacts were used, obtaining an average contact resistance of 0.6 Ohm*mm. The T−shaped Ni/Au−gates were defined by electron−beam lithography with a minimum gatelength of 0.15 µm. A scanning electron microscope image of the T−gate in the source drain area is shown in Fig. 4. All devices were passivated by a 100 nm thick SiN layer and multi−finger transistors were fabricated using first level metal interconnects and galvanic Au air bridges. The quality of the grown epitaxial layers and the subsequent processing technology is confirmed by CW load pull measurements at 2 GHz and 40 GHz (Fig. 5 and 6, respectively). Results from a device with 2 mm gatewidth and a gatelength of 300 nm are shown in Fig. 5. A linear gain of 23 dB, a maximum output power of 11.6 W yielding 5.8 W/mm, and a power added efficiency beyond 55 % are obtained under CW operating conditions. For a 150 nm GaN/AlGaN HEMT with a gatewidth of 8*60 µm, a linear gain beyond 5.5 dB, a maximum output power of 0.86 W yielding 1.8 W/mm, and a maximum PAE beyond 10 % are achieved (Fig. 6). The value of 0.86 W (1.8 W/mm) obtained for a single device at 40 GHz is, to our knowledge so far, the highest CW output power achieved with AlGaN/GaN based HEMT technology. Even at 40 GHz, an advantage of at least a factor of 3 in power density is gained with GaN technology in comparison to the mature GaAs PHEMT process [6].

3. LED and laser devices

Blue light emitting diodes (LEDs) were the first devices to be realized from group III−nitride compound semiconductors, after Amano et al. solved the problem of viable p−type doping [7]. In the last couple years GaN based LEDs covering the spectral window from green to near UV, are extending their range of application, including traffic signals, display and automotive application, environmental protection or even general lightning. The key advantages of these solid state light sources are lower energy consumption, long device lifetime and mechanical robustness. In lightning applications white LEDs are expected to outperform both incandescent and fluorescent light sources within the next decade. While single chip white LEDs − using a blue LED chip and a yellow phosphor converter − are already commercially available, white LEDs using a violet or UV pump LED and a tri−phosphor blend, which are expected to have an improved color rendering, are currently still under development. A prerequisite for use of these LEDs in general lightning application, however, is a further increase in the efficiency of the LED chips.

Since the first demonstration of a III−N based blue laser diode (LD) by Nakamura et al. in 1996 [8], several other groups including Sony, Xerox or Osram have announced the successful fabrication of blue/violet laser devices [9−11]. Such short wavelength semiconductor diode lasers will find a variety of applications including high density optical data storage (DVD−RAM / Blue Ray Disk), laser printing, spectroscopy, sensing and projection displays. Ultra high density optical data storage in DVD systems with a capacity exceeding 10 gigabytes is one of the key applications of violet light emitting diode lasers. Unfortunately many of these lasers still suffer from short lifetime due to the high density of dislocation in the layers structure resulting from the large lattice mismatch between GaN and the substrate. The reliability can be significantly improved by using epitaxially lateral overgrown (ELOG) GaN [12, 13] on sapphire or even the epitaxial growth of the laser structure on freestanding GaN substrates. Nagahama (Nichia) demonstrated laser devices with an estimated lifetime of 15000 hours under 30 mW CW operation at 60 °C [14].

a) Epitaxy of (AlInGa)N based LEDs for the fabrication of white LEDs

Layer sequences for violet and near UV emitting (AlInGa)N based LEDs were grown by low pressure MOVPE, both in our single and multiwafer reactor on conventional (unpatterned) 2” sapphire substrates. The layer structure presented in Fig. 7 consists of of 25 nm LT GaN nucleation layer, a 2000 nm undoped GaN buffer, a 1500 nm Si−doped ([Si]=1E19 cm^{-3}) n−contact layer, the active layer with an InGaN/GaN single or multiple quantum wells followed by a thin AlGaN:Mg electron blocking layer and the 200 nm thick Mg−doped ([Mg]=0.7..1.5E20 cm^{-3}) p−GaN contact layer. After the epitaxial growth the wafers were characterized by on wafer

elelectroluminescence (EL) measurements. Indium contacts are used to connect the p− and n−type GaN layers for rapid testing. Fig. 8 shows the EL output power of such an LED as a function of drive current, exceeding 3 mW @ 20 mA with a peak wavelength of l = 395 nm.

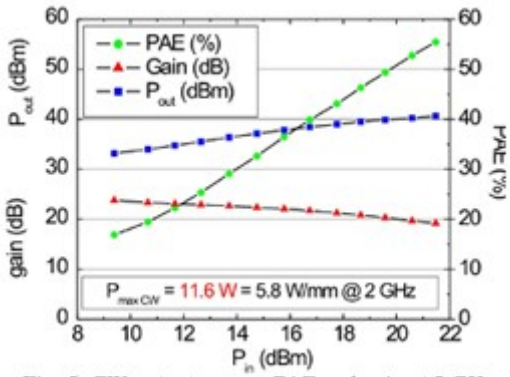

Fig. 5: CW output power, PAE and gain at 2 GHz for a 300 nm GaN/AlGaN HEMT on SiC with a gatewidth of 10x200 µm. V_{DS} = 35 V.

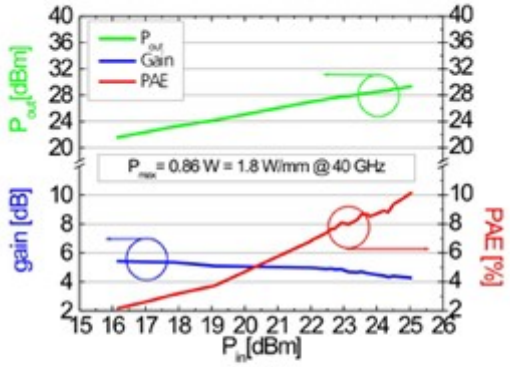

Fig. 6: Output power, PAE, and gain of a Wg = 480 µm AlGaN/GaN HEMT measured for V_{DS} = 30 V at 40 GHz

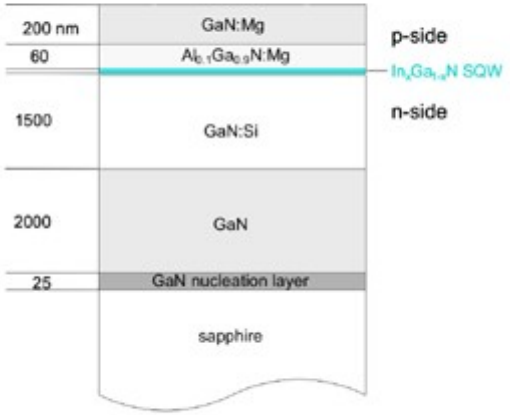

Fig. 7: Schematic layer sequence of an InGaN/GaN based SQW-LED structure grown by MOVPE for the fabrication of of near UV/violet

In order to realize luminescence converting (LUCO) LEDs, the above described and characterized epitaxial layer sequences were processed into mesa LEDs by standard optical lithography and chemically assisted ion beam etching (CAIBE). Electrical contacts to the n− and p−GaN contact layers were fabricated by lift−off technique, using Ti/Al/Ni/Au and Ni/Au as the n− and p−contact metalizations, respectively.

Several alternative approaches exist towards the realization of white emitting single−chip LEDs based on the principle of luminescence conversion. The so far most widely used approach combines a blue emitting (AlGaIn)N based LED chip with a yellow emitting YAG:Ce phosphor, yielding white light by additive color mixing when the relative intensities of the blue and yellow light component are adjusted appropriately. This approach has certain advantages because of its simplicity and its good overall power efficiency, as only one of the two primary colors is generated by luminescence conversion, thus limiting conversion losses due to Stokes shift. On the other hand the range of color coordinates, which can be covered by this approach, as well as the color rendering achieved, are limited.

To overcome these shortcomings, a violet/UV emitting LED chip is used as pump light source, whose short wavelength emission is not to be perceived by the human eye. The LED chip then excites a blend of three phosphors, converting the pump light into blue, green and red light (RGB−conversion), respectively [15]. This way, for a homogenous tri−color phosphor blend, a change in optical path length affects only the total amount of light converted, and thus the overall light intensity, and not the color coordinates as is the case for the more simple blue/yellow mixing LED. On the other hand this approach is particularly demanding with respect to the required optical properties of the phosphors employed. Using near−UV emission in the 390 to 400 nm wavelength range to reduce losses in overall conversion efficiency by minimizing the quantum deficit, requires a blue emitting phosphor with a particularly small Stokes shift between absorption and emission, while maintaining a high conversion efficiency, and a red−emitting compound with a particularly large Stokes shift for direct pumping by the LED rather than by the emission of the blue phosphor. While ensuring the best quality of white light emission in terms of color tuning, color rendering, and independence of color impression on viewing angle, a certain price will have to be paid in terms of overall power efficiency as all three color components of the white light are generated by luminescence conversion. Such UV pumped single−chip white LEDs with RGB tri−color luminescence conversion have been realized at the IAF in close collaboration with Osram Opto Semiconductors, Osram GmbH, and Siemens AG as industrial partners. Rare earth doped oxide and sulfide materials have been identified as appropriate inorganic RGB phosphors for optical pumping at wavelengths just below

the short−wavelength cut−off of the sensitivity of the human eye. Powders of these phosphors were dispersed in epoxy resin and detailed tests were carried out to determine the optimum phosphor concentrations with respect to conversion efficiency as well as with respect to the targeted color coordinates. Fig. 9 shows the EL spectrum of an UV−pumped tri−phosphor white LED employing a LED chip emitting at 394 nm. Chip and converter were encapsulated in epoxy using a standard 5 mm radial LED package. Besides residual emission from the pump chip, three phosphor−related emission bands centered at 460 nm, 550 nm, and 610 nm are resolved. The CIE color coordinates are x=0.365 and y=0.359 at an injection current of 20 mA, resulting in a color temperature of 4300 K. These parameters are those of a warm white hue, which cannot be generated by single−phosphor blue/yellow LEDs. Further optimization of the individual phosphors and of the phosphor blend will be required to improve the overall conversion efficiency.

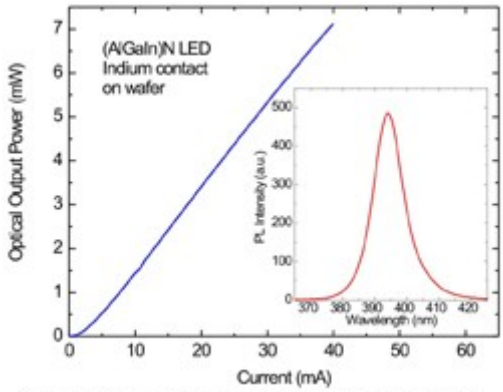

Fig. 8: Optical output power vs. current characteristic for an (AlGaIn)N LED emitting at l = 395 nm. The measurement was performed on wafer with Indium contacts. The corresponding electroluminescence spectrum is displayed in the inset

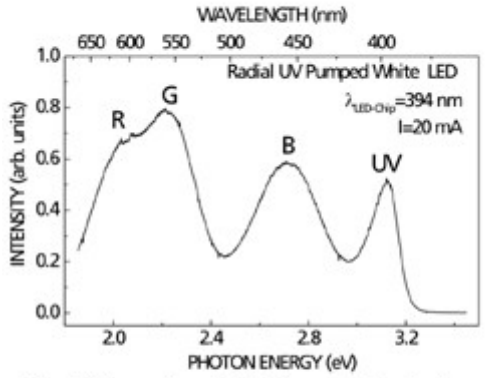

Fig. 9: EL spectrum of a UV-pumped tri-phosphor luminescence converting LED. Emission of the LED chip is centered at 394 nm. Emission from the phosphor blend in the red, green, and blue portion of the visible spectrum are indicated by R, G, and B, respectively

b) Blue laser diodes

The approach adopted by the Fraunhofer IAF for the fabrication of short wavelength diode lasers is based on the MOVPE growth of appropriate (AlGaIn)N layer sequences on 2” sapphire substrates. Based on our blue/violet LED structure, the layer sequence has been modified appropriately for the realization of the laser structure. The active region is composed of GaInN/GaN single or multiple QWs with an AlGaN electron barrier towards the p−contact, embedded between n− and p−doped GaN separate confinement layers and n− and p−doped AlGaN cladding layers. Using c−plane sapphire substrate rules out the use of conventional cleaving to form the laser mirrors. Thus mirrors are prepared by chemically assisted ion beam etching (CAIBE) in conjunction with a resist mask defined by photolithography. A schematic view of an (AlGaIn)N based ridge waveguide diode laser on insulating sapphire substrate is shown in Fig. 10, featuring etched mirror facets and a mesa etch for n−contact formation. A typical epitaxial structure for short wavelength diode lasers realized on sapphire substrates is shown in Fig. 11.

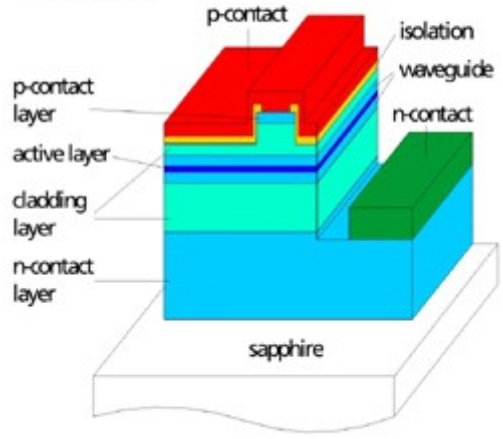

Fig. 10: Schematic view of an (AlGaIn)N based ridge waveguide diode laser on sapphire substrate with etched mirror facets

Pulsed output power vs. current characteristics of a series of 4x500 μm^2 ridge waveguide laser devices on sapphire fabricated from different epitaxial series are shown in Fig. 12. There is a clear reduction in threshold current with increasing sample number from (a) to (e), reflecting the progress achieved in epitaxial layer design and MOVPE growth. The lowest threshold current density measured for a 4x500 μm^2 device is 13.9 kA/cm^2 , which corresponds to a threshold current of 279 mA. An extrapolation of the best values of Ith towards infinite cavity length yields $I_{th,oo}$ = 6.3 kA/cm^2 . The slope efficiency amounts h = 415 mW/A per facet and the wavelength of the emitted laser light is l = 411 nm. The characteristic temperature T0 and T1, describing the temperature dependence of the threshold current and the slope efficiency, respectively, are 165 K and 210 K. All these data apply to devices without reflective facet coating and have been measured on wafer in pulse mode (200 ns pulse width, 0.2 % duty cycle) at 15 °C. Future work will focus on further lowering of threshold current and operating voltage as well as on a reduction of the defect density

by using appropriate GaN substrates, a necessity for long lived diode lasers.

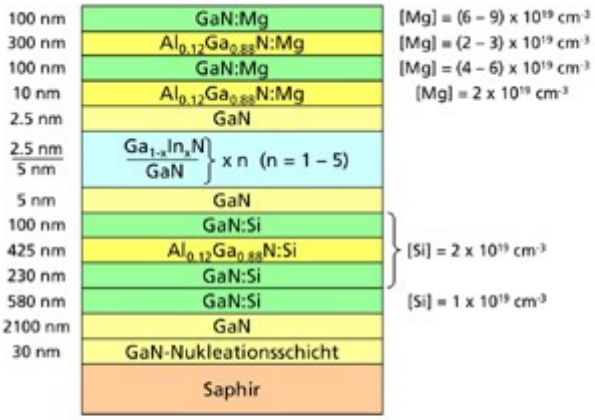

Fig. 11:. Typical epitaxial layer sequence of an (AlGaIn)N based MQW diode laser

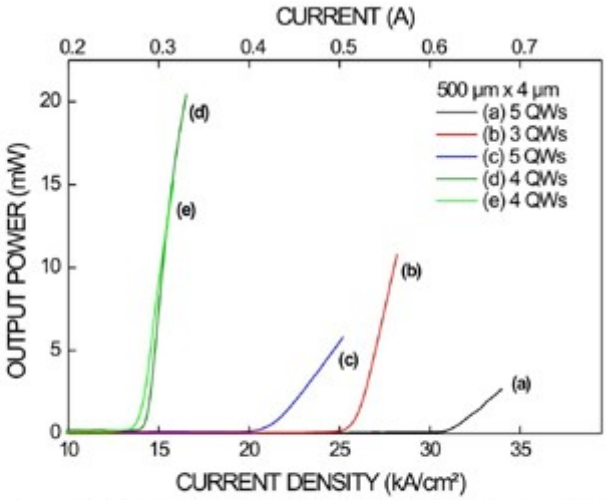

Fig. 12: Typical output power vs. current characteristic of 5 lasers from different laser MQW structures. The improvement in device performance is a result of the continuous structure optimization from (a) to (e)

Conclusions

We have demonstrated the growth of GaN/AlGaN heterostructures by MOVPE for power HEMT applications. The electrical properties of the 2−DEG as well as the excellent uniformity of the wafers are ideal prerequisites for reproducible high yields for device fabrication. The quality of both epitaxy and processing is confirmed by CW load pull measurements at 2 GHz and 40 GHz with output power of 11.6 W and 0.86 W, respectively. Near UV emitting (AlInGa)N based LEDs covering the 380 to 430 nm wavelength range have been developed as pump sources for the fabrication of white LEDs. The optical output power of the near UV LED was up to 3 mW @ 20 mA at l = 395 nm. Tricolor LUCO white LEDs have been produced and characterized and show superior color quality to that of YAG:Ce based white LEDs. Short wavelength diode laser structures have been grown on conventional 2” sapphire. Devices with uncoated mirror facets show lasing at l = 411 nm with a minimum threshold current of 278 mA, which corresponds to a threshold current density of 13.9 kA/cm^{-2} for the 500 µm*4 µm device.

Acknowledgement

The authors acknowledge support of the German Federal Ministry of Education and Research (BMBF) and of the Federal Ministry of Defence (BMVg).

References

[1] Y.−F. Wu, B. P. Keller, S. Keller, P. Kapolnek, P. Kozodoy, S. P. DenBaars, and U. K. Mishra, Solid State Electron. 41, 1569−1574 (1997)
[2] M. S. Shur, Solid State Electron. 42, 2131−2138 (1998)
[3] H. Morkoc, A. Di Carlo, and R. Cingolati, Solid State Electron. 46, 157−202 (2002)
[4] O. Ambacher, J. Smart, J. R. Shealy, N. G. Weimann, K. Chu, M. Murphy, R. Dimitrov, L. Wittmer, M. Stutzmann, W. Rieger, and J. Hilsenbeck, J. Appl. Phys. 85 3222−3233 (1999)
[5] J. Wagner, H. Obloh, M. Kunzer, M. Maier, K. Köhler, and B. Johs, J. Appl. Phys. 89, No. 5 2779 (2001)
[6] R. Quay, R. Kiefer, F. van Raay, H. Massler, S. Ramberger, S. Müller, M. Dammann, M. Mikulla, M. Schlechtweg, and G. Weimann, Int. Electron Dev. Meeting, San Francisco, session 28, (2002).
[7] H. Amano, I. Akasaki, T. Kozawa, K. Hiramatsu, N. Sawak, K. Ikeda, and Y. Ishi, J. Lumin. 40−41, (1988)
[8] S. Nakamura, M. Senoh, S. Nagahama, N. Iwasa, T. Yamada, T. Matsuhitah. Kiyoku, and Y. Sugimoto, Jpn.

Appl. Phys. 35, L74 (1996)
[9] M. Ikeda and S Uchida, phys. stat. sol. (a) 194, No.2, 407−413 (2002)
[10] W. S. Wong, M. Kneissl, P. Mei, D. W. Treat, M. Teepe, and N. M. Johnson, Appl. Phys. Lett. 78, 1198 (2001)
[11] V. Kümmler, G. Brüderl, S. Bader, S. Miller, A. Weimar, A. Lell, V. Härle, U.T. Schwarz, N. Gmeinwieser, and W. Wegschneider, phys. stat. sol. (a) 194, No.2, 419−422 (2002)
[12] A. Usui, H. Sunakawa, A. Sakai, and A. Yamaguchi, Jpn. J. Appl. Phys. 36 L899−L902 (1997)
[13] O.H. Nam, M.D. Bremser, T. Zheleva, and R.F. Davis Appl. Phys. Lett. 71, 2638 (1997)
[14] S. Nagahama, N. Iwasa, M. Senoh, T. Matsushita, Y. Sugimoto, H. Kiyoku, T. Kozaki, M. Sano, H. Matsushita, H. Umemoto, K. Chocho, and T. Mukai, Jpn. J. Appl. Phys. 39, L647−L650 (2000)
[15] U. Kaufmann, M. Kunzer, K. Köhler, H. Obloh, W. Pletschen, P. Schlotter, R. Schmidt, J. Wagner, A. Ellens, and M. Kobusch, phys. stat. sol. (a) 188, 143 (2001)